Desalination and Water Treatment
www.deswater.com
doi: 10.1080/19443994.2014.924880

55 (2015) 1240–1252
July

Taylor & Francis
Taylor & Francis Group

Adsorption competition of Cu(II) ion in ionic pair and multi-metal solution by ionic imprinted amino-silica hybrid adsorbent

Buhani[a,*], Narsito[b], Nuryono[b], Eko Sri Kunarti[b], Suharso[a]

[a]*Faculty of Mathematic and Natural Sciences, Department of Chemistry, University of Lampung, Jl. Soemantri Brojonegoro No. 1, Bandar Lampung, Indonesia, Tel. +62721704625; Fax: +62721702767; email: buhani_s@yahoo.co.id (Buhani)*
[b]*Faculty of Mathematic and Natural Sciences, Department of Chemistry, Gadjah Mada University, Yogyakarta, Indonesia*

Received 16 April 2013; Accepted 9 May 2014

ABSTRACT

It was carried out the synthesis of the Cu(II) ionic imprinted polymer (Cu(II)-IIP) material of amino-silica hybrid via sol-gel process using a tetraethyl-orthosilicate precursor and an active compound 3-aminopropyltrimetoxyslane. Adsorption process of Cu(II) ion on non-imprinted ionic (NIP) material and Cu(II)-IIP follows pseudo-first-order kinetics model with the value of adsorption rate constants (k_1) 0.030 and 0.058 L/min and Langmuir adsorption isotherm with the value of adsorption capacity 29.556 and 71.400 mg/g, respectively. Adsorption competition data in ion pair solution of Cu(II)/Ag(I), Cu(II)/Zn(II), Cu(II)/Ni (II), and Cu(II)/Cd(II) showed that the Cu(II)-IIP adsorbent was more selective than NIP with value of selectivity coefficient (α) > 1. A tendency of metal ion adsorbed in multi-metal solution follows this order: Ca(II) < Cd(II) < Ni(II) < Zn(II) < Ag(I) < Cu(II). The Cu(II)-IIP is stable chemically and it can be reused for adsorption of Cu(II) ion in solution without reduction of its capacity.

Keywords: Cu(II) ionic imprinted; Selective adsorption; Sol-gel; Amino-silica hybrid

1. Introduction

Environmental pollution by heavy metals derived from human activities from industry, mining, and metallurgy gives negative effects on ecosystem and human living. This is caused by heavy metal characteristics which could not be degraded in environment and could be harmful to a variety of living species. Besides their toxic and harmful effects to organisms living in water, heavy metals also accumulate throughout the food chain, and may eventually affect human beings [1,2].

One of heavy metals which are essential needed by human beings is Cu metal. Cu metal is needed by human beings for Fe metabolism in hemoglobin, but in high concentration, it will be toxic and accumulate in the human body. For these reasons, some works were performed to reduce the existence of heavy metals in environment, especially Cu metal. Several researches were carried out to minimize spreading out of Cu metal in environment with development of an adsorbent to adsorb Cu metal in solution [2–5].

One of selective adsorbent synthesis techniques which are more developed is an ionic imprinting technique. This technique can be used to separate selectivity and to preconcentrate trace metals. The main application of the ionic imprinting polymer is

*Corresponding author.

preconcentration through a solid-phase extraction (SPE) process from analyte which exist in trace concentration and separation from other analytes which are exist together or complex matrix, resulting selectivity upon analyte of clean-up process in the environment that cannot be reached by a conventional method [6]. The ionic imprinting technique can raise the selectivity because metal ions can play a role as a template forming polymer through the imprinting technique [7–10]. In addition, a cost of the ionic imprinted polymer (IIP) material is relatively low and it can be kept at room temperature for a long time.

Several researches have been done to produce a selective ionic imprinted material upon adsorption of Cu(II) ion in aqueous solution in a preconcentration and a separation process such as ion-imprinted polymer based on salen-Cu complex [11], Double-imprinted polymer [12], Cu(II)-imprinted polymethacrylic microbeads [13], copper-imprinted porous polymer microbead [14], Cu^{2+}-imprinted microporous polymer particle [15], chitosan/*Sargassum* sp. composite by an innovative ion-imprinted technology [16].

In this research, it has been performed simultaneously the synthesis of ionic Cu(II)-imprinted material derived from an amino-silica hybrid through a sol-gel process using a tetraethyl-orthosilicate (TEOS) precursor. A simultaneous process of sol gel and an ionic imprinting was performed to obtain more homogeneous ionic imprinted material in preparing optimal ionic imprinted cavities [17,18]. In addition, the ionic imprinted material obtained will have high-adsorption selectivity and capacity against a target metal ion. The functional group immobilized on silica gel was $–NH_2$ from an active compound of 3-aminopropyltrimethoxysilane (APS). The addition of an amine group is expected to increase a silica capacity on adsorbing metal ion because N atom on the amine group is good electron donor (ligand) to interact with Cu(II) ion. The material produced used as selective adsorbent of Cu (II) ion in mono and multi-metal solution through series of adsorption process as well as chemical stability test and reusability of the adsorbent.

2. Experimental methods

2.1. Materials

APS is obtained from Aldrich. The TEOS, ethanol, $CdCl_2{\cdot}H_2O$, $ZnCl_2$, $NiCl_2{\cdot}6H_2O$, $CuCl_2{\cdot}2H_2O$, $CaCl_2$, AgCl, Na_2EDTA, KNO_3, $HONH_2HCl$, CH_3COOH, and HNO_3 used are commercial products of Merck, Germany. NaOH, HCl, and NH_4OH were purchased from Alba Chemical.

2.2. Synthesis of Cu(II) IIP from amino-silica hybrid

The synthesis of Cu(II) IIP with the active compound of APS, the solution which will be interacted was divided into two parts, namely, solution A and solution B. The solution A was prepared by adding two drops of HCl until pH of 2 to a mixture of 5 mL TEOS and 5 mL water in plastic container and stirring with magnetic stirrer for 30 min. The solution B was prepared by dissolving 0.17048 g $CuCl_2{\cdot}2H_2O$ and in 5 mL ethanol, then added 1 mL 3-APS. Solution A and B were mixed by stirring using a magnetic stirrer for 30 min. A gel formed was kept for a night and rinsed with a mixture of water–ethanol 60/40% (v/v) followed soaked with 0.1 M Na_2EDTA solution for 24 h and followed stirring with 0.5 M HCl for 30 min. Further, the material obtained was dried in an oven (Fisher Scientific) for 6 h at temperature of 60°C. The resulted material was ground and sieved, of 200 mesh size selected as experimental material. NIP was also prepared under similar experimental conditions without adding $CuCl_2{\cdot}2H_2O$.

The material was characterized with infrared (IR) spectroscopy (Prestige—21 Shimadzu, Made in Japan). Data of N_2 gas adsorption-desorption isotherms were obtained using a surface area analyzer Quantachrome Nova 1200e, and pore size distributions were calculated using the Barret–Joyner–Halenda model on the adsorption branch. The metal solution was analyzed using an atomic absorption spectrophotometer (AAS; Model Perkins Elmer 3110, Made in USA). A scanning electron microscopy (SEM) and energy-dispersive X-ray analysis (EDX) (JSM) 6360 LA) were used for identification of surface morphology and element composition.

2.3. Sorption experiment

The effect of pH on the sorption of Cu(II) was tested by mixing 50 mg of the prepared material and 20 mL 100 mg/L Cu(II) in buffer solution at various pH for 1 h. Adsorption kinetics of Cu(II) on the prepared materials were performed in similar way as previous interaction at pH optimum and various contact times.

The adsorption capacity, the distribution ratio, the selectivity coefficient, and the relative selectivity coefficient were calculated using the following equations:

$$q = (C_o - C_e)V/W \tag{1}$$

$$D = q/C_e \tag{2}$$

$$\alpha M_1 M_2 = D_{\mathrm{Cu}}/D_M \tag{3}$$

$$\alpha_r = \alpha_i/\alpha_n \tag{4}$$

where q represent the adsorbed metal ion (mg/g), C_o and C_e represent the initial and final concentration of metal ions (mmol/L), respectively, W is the mass of adsorbent (g), V is the volume of metal ion solution (L), D is the distribution ratio (L/g), α is the selectivity coefficient, D_{Cu} and D_M represent the distribution ratios of Cu(II) to Ni(II), Cd(II), Zn(II), or Ag(I). α_r is the relative selectivity coefficient, α_i and α_n represent the selectivity factor of imprinted adsorbent and NIP, respectively.

The adsorption rate was determined based on kinetic pseudo-first-order (Eqs. (5) and (6)) and pseudo-second-order (Eqs. (7) and (8)). Evaluation of these kinetics models was performed using Eqs. (9) and (10). Similar work was carried out by varying the concentrations of Cu(II) to determine the adsorption capacity calculated using Freundlich and Langmuir equation (Eqs. (11)–(14)).

Selectivity of adsorption was evaluated based on the data of binary competitive metal ion adsorption for Cu(II)/Cd(II), Cu(II)/Ni(II), Cu(II)/Zn(II), and Cu (II)/Ag(I) in aqueous solution at pH of 6. The Cu(II)-IIP adsorbent (50 mg) was equilibrated with 20 mL of the buffer solution containing 0.5 mmol/L of Cu(II) and 0.5 mmol/L of Cd(II), Ni(II), Zn(II), and Ag(I).

Multi-metal adsorption–desorption was performed using SPE column. The column and filter were cleaned using water and alcohol 70%. An amount of 0.5 g material was loaded into column and then flowed with multi-metal solution containing each 0.5 mmol/L of Cu(II), Cd(II), Ni(II), Zn(II), Ag(I), and Ca(II). The volume of each stage was 10 mL. The adsorbed metal ions were eluted by water followed by Na_2EDTA 0.1 M and HCl 0.5 M solution.

2.4. Reusability

Metal ion adsorbed on material was released in a batch system from material by stirring for 30 min with solution of 0.1 M HCl and Na_2EDTA 0.1 M. After washed with water up to neutral condition, the material was reused to adsorb Cu(II) ion with batch method up to nine times.

3. Results and discussion

3.1. Synthesis of Ionic imprinted polymer for Cu(II)

Preparation of the Cu(II)-IIP material was performed through several steps. First step is a complex formation between Cu(II) ion and APS in ethanol. Second step is a silica net formation from TEOS precursor to produce Cu(II)-amino polymer. The last step is a releasing of Cu(II) ion as a template of polymer to form ionic imprinted cavities. The reaction mechanism model proposed in the synthesis of Cu(II)-IIP from amino-silica hybrid is displayed in Fig. 1.

3.2. Characterization of the adsorbents

Fig. 2 describes an IR spectrum of silica gel (SG), NIP, polymer adsorbing copper (Cu-P), and Cu(II)-IIP sorbent. From this figure, the bands around 1,087.85 and 964.41 l/cm represent stretching vibration of Si–O–Si and Si–OH, respectively. The bands at 794.67 and 470.63 l/cm were predicted from vibration of Si–O. The characteristic differences between SG and Cu(II)-IIP, Cu-P and Cu(II)-IIP materials were presented by appearing the new band at 2,939.52 l/cm which is a representation of stretching vibration of CH_2 and band characteristic of $-NH_2$ at 1,640–1,550 l/cm [19–21], and at 3,448.72 l/cm derived from asymmetric vibration $-NH_2$ [22]. These facts prove that the immobilization of amino group in NIP, Cu-P, and Cu(II)-IIP has occurred.

Surface areas for NIP and Cu(II)-IIP were determined through BET equation and the results obtained were 87.873 and 38.536 m^2/g, respectively. These values are lower than SG (199.801 m^2/g). The decreasing of surface area after incorporation of organic groups can be easily explained due to the fact that presence of pendant group blocks partially the adsorption of nitrogen molecules on the surface, resulting in a decreasing of surface area [23,24].

The nitrogen adsorption–desorption isotherms for NIP and Cu(II)-IIP are shown in Fig. 3. For the NIP and the Cu(II)-IIP, the isotherms are type IV according to the IUPAC classification and have a H1 hysteresis loop representing mesopores. For all isotherms, the adsorbate volumes increase sharply upon (P/P_o) at around 0.6 showing nitrogen caviler condensation in orderly mesoporous structures. Hysteresis loop at Cu (II)-IIP is weaker than NIP because of decreasing of porous volume after functionalization and ionic imprinting process [24,25].

SEM–EDX analysis result of NIP, Cu-P, and Cu(II)-IIP (Fig. 4) shows that surface morphology of Cu-P (Fig. 4(b)) appears brightest than surface morphology of NIP (Fig. 4(a)) and Cu(II)-IIP (Fig. 4(c)). This is caused on Cu-P existed Cu ion producing brighter color because of higher accelerating (high atomic number of Cu) on Cu-P material. This fact was supported by EDX spectrum on NIP material (Fig. 4(d)) showing only existence of silica, carbon, nitrogen, and oxygen. While, in Fig. 4(e) for Cu-P, besides the elements of

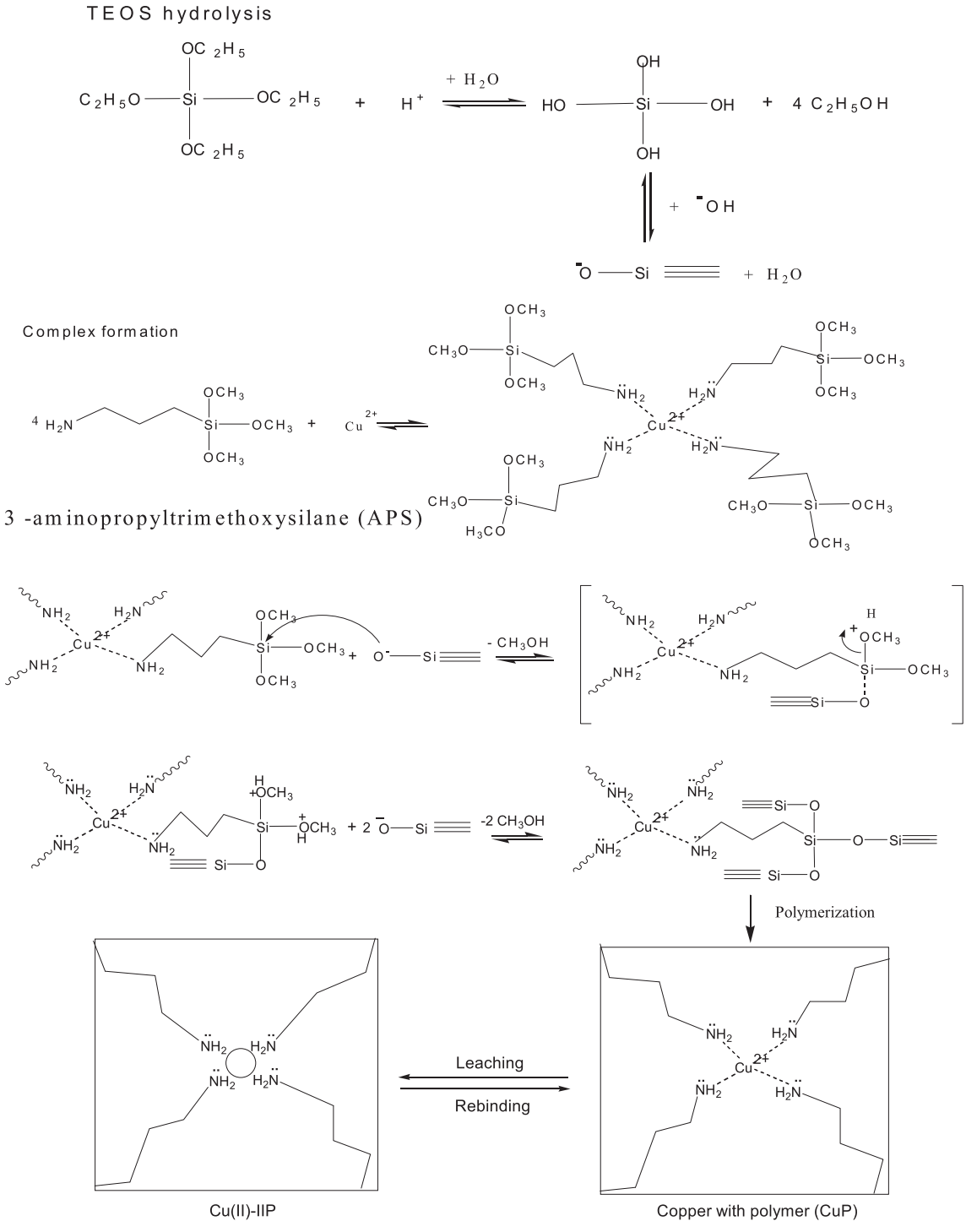

Fig. 1. Mechanism of Cu(II)-IIP synthesis proposed.

silica, carbon, nitrogen, and oxygen, the spectrum shows the existence of Cu which is metal ion used as template. Cu(II) ion will be released to produce ionic imprinted cavities on Cu(II)-IIP (Fig. 4(f)).

3.3. Parameters influencing adsorption

Interaction between metal ion (adsorbate) and adsorbent on adsorption process is influenced by several factors such as adsorbent dose, system pH,

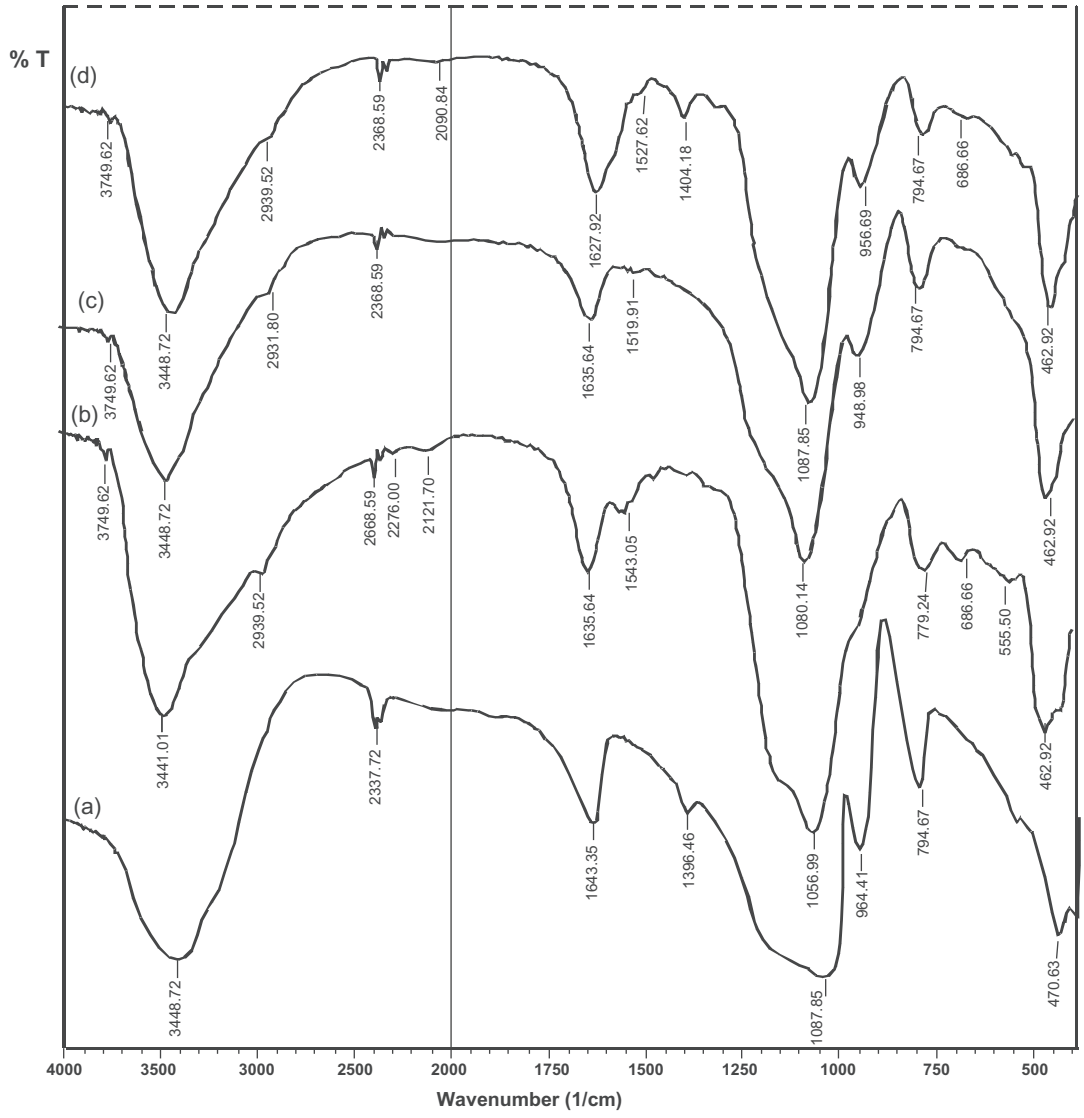

Fig. 2. IR spectrum of (a) silica (SG) from TEOS; (b) NIP; (c) CuP; and (d) Cu(II)-IIP.

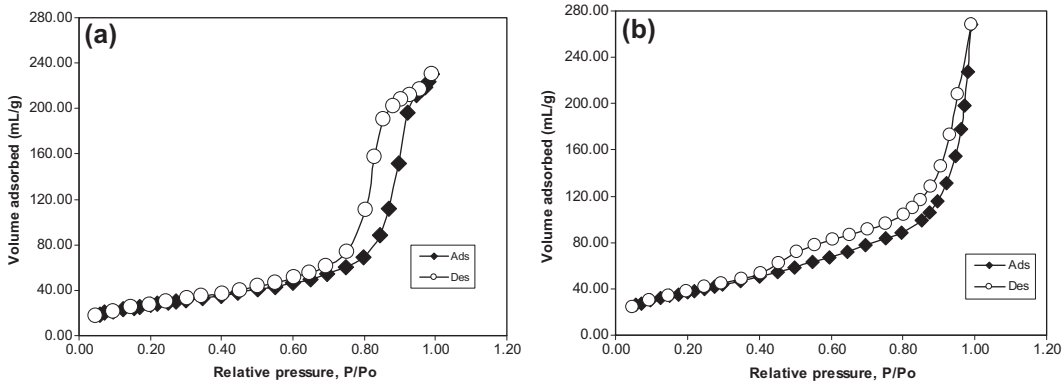

Fig. 3. Nitrogen adsorption–desorption isotherms of (a) NIP and (b) Cu(II)-IIP.

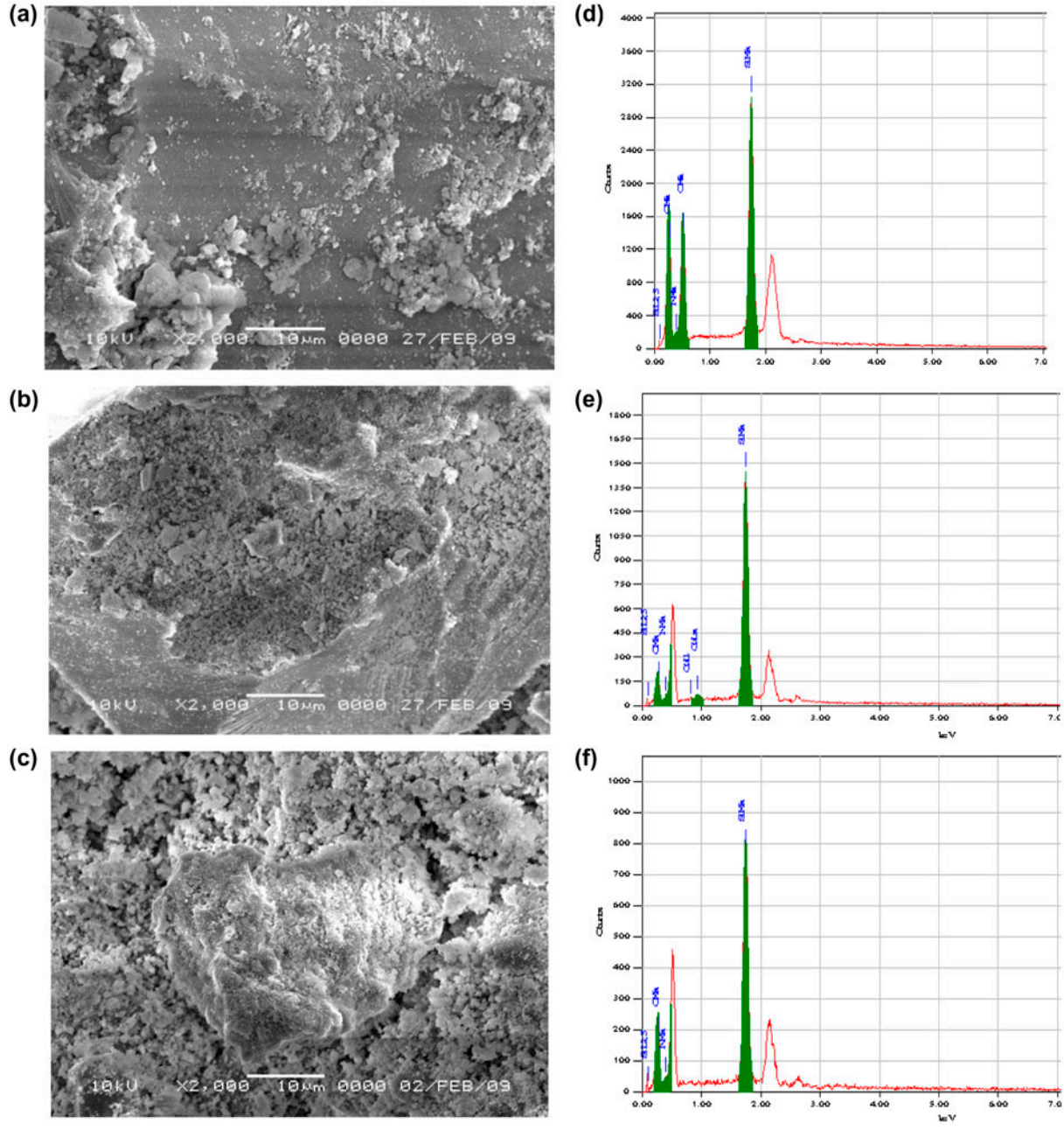

Fig. 4. SEM of (a) NIP, (b) Cu-P, (c) Cu(II)-IIP and EDX spectrum of (d) NIP, (e) Cu-P, and (f) Cu(II)-IIP.

interaction time, metal ion concentration, and temperature. Effect of these parameters on adsorption of Cu (II) ion by NIP and Cu(II)-IIP can be seen in Fig. 5.

3.3.1. Effect of adsorbent dose

To investigate the effect of adsorbent dose, an amount of NIP adsorbent and Cu(II)-IIP (10–50 mg) was interacted with 20 mL of 100 mg/L Cu(II) ion solution. It can be seen in Fig. 5(a), Cu(II) ion adsorption raised with increasing of adsorbent dose and reached to plateau at the appropriate dose of 50 mg adsorbent. This fact shows that addition of adsorbent dose increases amount of metal ion adsorbed.

3.3.2. Effect of pH

The effect of pH was studied by interacting Cu(II) ion with the NIP and Cu(II)-IIP in batch system at various pHs (3–8) (Fig. 5(b)). At low pH (pH 3.0), the Cu(II)

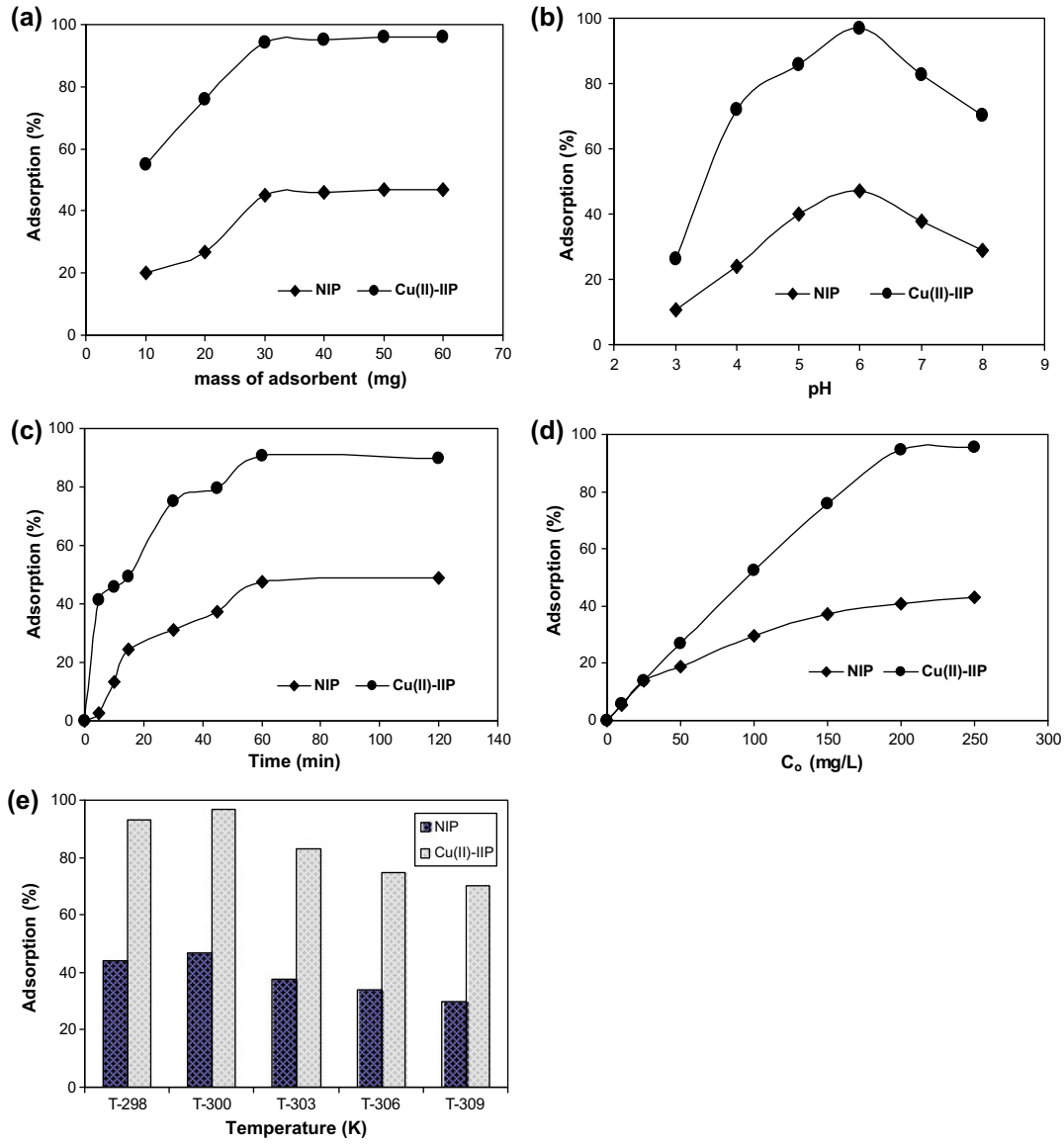

Fig. 5. Effect of adsorption from (a) adsorbent dose, (b) initial pH, (c) performing time, (d) initial concentration of Cu(II) ion, and (e) temperature toward sorption of Cu(II) on NIP and Cu(II)-IIP; sample volume of 20 mL.

was adsorbed very small. At this acid condition, amine group ($–NH_2$) is protonated to be NH_3^+ so that the interaction between Cu(II) ion and active sites on the adsorbent tends to be rejected electrostatically causing weak bonding between the Cu(II) ion and adsorbent [26].

At pH 6, the adsorption process of Cu(II) ion adsorption on the NIP and the Cu(II)-IIP reaches optimum condition because the active sites on the material ($–NH_2$ group) are in the neutral condition. Therefore at this condition, the adsorbent can play role as electron pair donor and result interaction between the Cu(II) ion and adsorbent active sites. At pH 7, Cu(II) ion concentration adsorbed starts to decrease because the ion starts to precipitate as $Cu(OH)_2$ causing decreasing of Cu(II) ion in solution. In this condition, the precipitation process is more dominant than the adsorption process [12].

3.3.3. Effect of interaction time

In this research, it was studied effect of the interaction time on Cu(II) ion and Cu(II)-IIP compared with NIP material to investigate an optimum interaction time (Fig. 5(c)). In Fig. 5(c), it can be seen that generally, Cu(II) ion adsorption on Cu(II)-IIP runs relatively

quick. At first 15 min, the adsorption increases very sharply. After second 15 min, the adsorption runs slowly and it is constant at interaction time of 60 min. At this 60 min of interaction time, it occurred equilibrium and increasing of interaction time does not give increasing of Cu(II) ion amount adsorbed significantly.

3.3.4. Effect of metal ion concentration

Fig. 5(d) shows Cu(II) ion adsorption isotherm model on Cu(II)-IIP with various initial concentrations. From the data obtained in this figure, it can be observed that Cu(II) ion adsorption increases with raising of metal ion concentration and at high-relative concentration, increasing of metal ion concentration is not followed with increasing of Cu(II) ion adsorption on Cu(II)-IIP significantly. These facts show that at high-relative concentration, Cu(II)-IIP active sites have been too full and their adsorption capacity has been maximum.

3.3.5. Effect of temperature

In Fig. 5(e), it can be seen that percentage of Cu(II) ion adsorbed by NIP and Cu(II)-IIP decreases with increasing of temperature from 298 to 309 K. It can be observed in generally from Fig. 5(e), percentage of metal adsorbed (%) decrease with increasing temperature. This shows that the adsorption is not favorable at higher temperature. This is possibly due to the exothermic effect of the surroundings during the adsorption process.

3.4. Adsorption kinetics

Pre-equilibrium kinetic profiles were identified in order to analyze the rate-limiting steps involved in the processes of adsorption of Cu(II) ions on NIP and Cu (II)-IIP. Pseudo-first and second-order models, the kinetic of total Cu(II) adsorption by NIP and Cu(II)-IIP (Fig. 6) was tested with respect to first-order model of Lagergren (Eqs. (5) and (6)) and second-order model (Eqs. (7) and (8)) [27,28]:

$$q_e = q_e(1 - e^{-k_1 t}) \tag{5}$$

$$\log(q_e - q_t) = \log q_e - \frac{k_1}{2.303} t \tag{6}$$

$$q_t = \frac{q_e^2 k_2 t}{1 + q_e k_2 t} \tag{7}$$

$$\frac{t}{q_t} = \frac{1}{k_2 q_e^2} + \frac{t}{q_e} \tag{8}$$

where q_t and q_e (mg/g) are total Cu(II) ions adsorption capacity at time t and at equilibrium, respectively, k_1 and k_2 are the first-order and second-order rate constants, respectively. Table 1 shows total Cu(II) ions adsorption rate constants (k_1 and k_2) and correlation coefficients calculated using linearized plots of Eqs. (6) and (8), respectively. These kinetics models were evaluated to determine the root mean squared error (*RMSE*) and Chi-square test (χ^2) [29,30] with these equations below:

$$RMSE = \sqrt{\left(\frac{1}{m-2}\right) \sum_{i=1}^{m} \left(q_{i,\exp} - q_{i,\mathrm{cal}}\right)^2} \tag{9}$$

$$\chi^2 = \sum_{i=1}^{m} \frac{\left(q_{i,\exp} - q_{i,\mathrm{cal}}\right)^2}{q_{i,\exp}} \tag{10}$$

where $q_{i,\exp}$ and $q_{i,\mathrm{cal}}$ were obtained from estimation and experiment data via adsorption isotherm equation, m is the number of observation in the experimental isotherm.

Adsorption process of Cu(II) ion on NIP and Cu(II)-IIP (Fig. 6 and Table 1) tends to follow the pseudo-first-order kinetic model, showed with the value of correlation coefficient (R^2), *RMSE*, and χ^2 which are best fitted to pseudo-second-order kinetic model. A smaller *RMSE* value indicates a better curve fitting, moreover, if the data obtained from the model are close to the experimental results, χ^2 will be a small number [30]. This fact proves that the adsorption process is very determined by an adsorbate factor (Cu(II) ion), while the adsorbent is a constant characteristic.

3.5. Adsorption of monometal

Data of Fig. 5(c) were evaluated using Freundlich and Langmuir adsorption isotherm equation [31], as well as using linear and non-linear parameters. Freundlich equation is equation empirically based on heterogeneous surface. General model linear and non-linear of Freundlich equation (Eqs. (11) and (12)) as follow:

$$q_e = \log K_f \, C_e^{\frac{1}{n}} \tag{11}$$

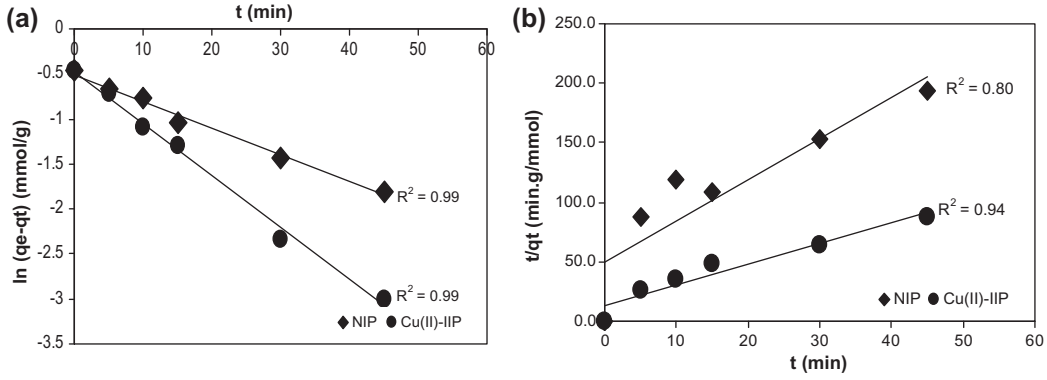

Fig. 6. Adsorption kinetic linear model of Cu(II) ion on NIP and Cu(II)-IIP (a) pseudo first order and (b) pseudo second order.

Table 1
Adsorption kinetic constant of Cu(II) ion on NIP and Cu (II)-IIP material, at pH of 6; Cu(II) initial concentration of 100 mg/L; sample volume of 20 mL; temperature of 27°C

		Materials	
	Parameters	NIP	Cu(II)-IIP
Experiments	$q_{e,\exp}$ (mg/g)	27.576	35.455
Pseudo-first-order	k_1 (1/min)	0.030	0.058
	$q_{e,\text{cal}}$ (mg/g)	28.085	34.248
	R^2	0.989	0.994
	RMSE	0.024	0.016
	χ^2	0.004	0.002
Pseudo-second-order	k_2 (g/mg min)	15.250	15.186
	$q_{e,\text{cal}}$ (mg/g)	18.363	42.572
	R^2	0.879	0.936
	RMSE	0.545	0.400
	χ^2	2.154	1.957

$$\log q_e = \log K_f + \frac{1}{n}\log C_e \tag{12}$$

with K_f is adsorption capacity factor, n is intensity factor with the value around 1–10.

Langmuir isotherm stated that on adsorbent surface, it is found a number of active sites which is comparable with surface area. Langmuir equation non-linear and linear (Eqs. (13) and (14)) are written as follow:

$$q_e = \frac{q_m K C_e}{1 + K C_e} \tag{13}$$

$$\frac{C_e}{q_e} = \frac{1}{q_m} K + \frac{C_e}{q_m} \tag{14}$$

where C_e (mg/L) is metal ion solution equilibrium concentration, q_e (mol/g) is metal ion adsorption capacity at equilibrium, q_m is adsorption capacity of adsorbent monolayer, and K is adsorption energy constant.

Non-linear parameter in Freundlich and Langmuir adsorption isotherm equation was applied in the adsorption isotherm data obtained. These non-linear procedures produce least squares or weighted least squares estimates of the parameters of a non-linear model. Correlation between q_e and C_e from both the adsorption isotherm models with non-linear and linear model was displayed in Figs. 7 and 8. Analysis results of adsorption isotherm parameters of Cu(II) ion adsorption by NIP and Cu(II)-IIP were listed in Table 2.

From Table 2, it can be known that adsorption isotherm model of Cu(II) ion on Cu(II)-IIP tends to follow Langmuir isotherm model with value of regression coefficient (R^2) higher than Freundlich isotherm model. This fact was also supported by the value of *RMSE* and χ^2 on Langmuir isotherm lower than Freundlich isotherm model. In this research, metal ion concentration used is high enough, until adsorption isotherm model fitted with the experiment result is Langmuir adsorption isotherm model [31]. In addition, it can be observed also that Langmuir adsorption isotherm parameters of Cu(II) ion adsorption process by NIP and Cu(II)-IIP fit using non-linear model. This case is shown with the value of *RMSE* and χ^2 of non-linear model smaller than the value of *RMSE* and χ^2 of linear model (Fig. 7).

Adsorption energy is determined based on Gibbs free energy equation [29,32] as shown in Eq. (15):

$$\text{Absorption energy} = \Delta G^\circ \text{ ads} = R \times T \ln K \tag{15}$$

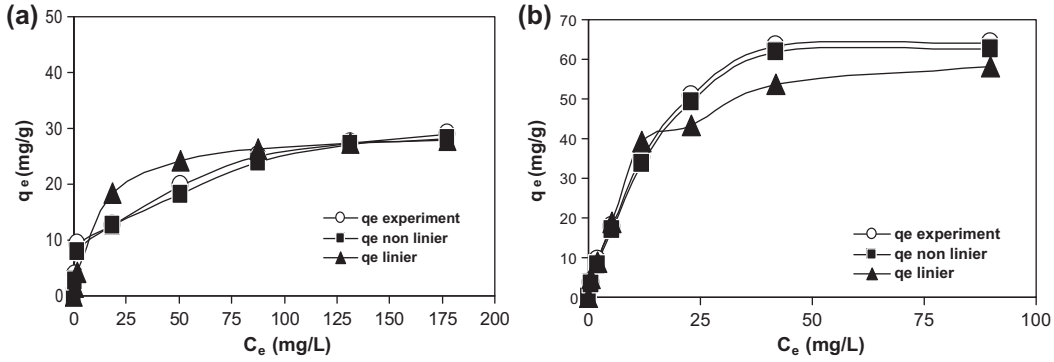

Fig. 7. Langmuir adsorption isotherm linear and non-linear model of Cu(II) ion on (a) NIP and (b) Cu(II)-IIP.

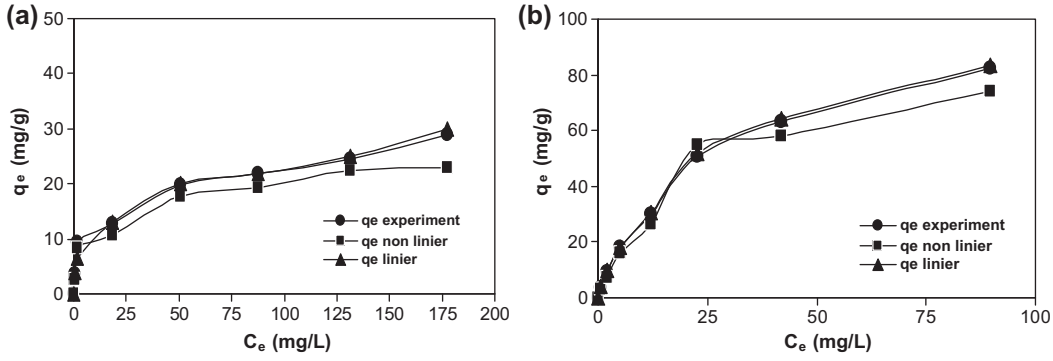

Fig. 8. Freundlich adsorption isotherm linear and non-linear model of Cu(II) ion on (a) NIP and (b) Cu(II)-IIP.

Table 2
Freundlich and Langmuir adsorption isotherm parameters of Cu(II) ion on NIP and Cu(II)-IIP at pH of 6; sample volume of 20 mL; temperature of 27°C

		Models			
		Linear		Non-linear	
	Parameters	NIP	Cu(II)-IIP	NIP	Cu(II)-IIP
Adsorption isotherm					
Freundlich	K_f (mg/g)	5.442	6.734	2.643	3.642
	n	3.031	1.727	3.830	2.517
	R^2	0.965	0.966	0.956	0.947
	RMSE	3.421	5.036	5.350	8.144
	χ^2	3.847	3.969	4.319	4.548
Langmuir	q_m (m/g)	29.556	71.400	28.456	74.012
	$K \times 10^3$ (L/mol)	5.775	6.921	4.045	13.516
	R^2	0.988	0.978	0.998	0.997
	RMSE	1.775	1.492	1.084	1.038
	χ^2	1.264	0.781	1.021	0.605

with E is adsorption energy (kJ/mol), R is universal gas constant (8.314 J/K mol), T is temperature (Kelvin), and K is adsorption equilibrium constant (Table 2).

Adsorption energy of Cu(II) ion on the NIP and the Cu(II)-IIP at temperature of 300 K is each 21.603 and 22.054 kJ/mol. This adsorption energy value is too

low to be considered as chemical bonding energy, but it is higher to be considered as physic induction [33]. Cu(II) ion interaction on the NIP and the Cu(II)-IIP adsorbent is classified into weak interaction because the lowest limit of chemical energy is 20 kJ/mol [34]. Thus, interaction among Cu(II) ions with NIP and Cu (II)-IIP is grouped as physical process and it occurs decreasing of randomness at solid/liquid interface during the adsorption of metal ions on adsorbent surface [35]. This shows that the adsorption process is stable on solid–liquid interface [4].

If the adsorption capacity data of Cu(II) ion on the Cu(II)-IIP is compared that reported in result of other researches about Cu(II) IIP as listed in Table 3, it can be seen that the Cu(II) adsorption capacity on the Cu (II)-IIP resulted is relatively higher than on other materials in adsorbing Cu(II) ion.

3.6. Competitive adsorption in ionic pairs and multi-metals

Competitive adsorption of Cu(II)/Cd(II), Cu(II)/Ni (II), Cu(II)/Zn(II), and Cu(II)/Ag(I) binary mixture Cu (II) ion was also investigated in a batch system. Although these ions posses a similar ionic radii (Ag(I) = 1.29, Cd(II) = 1.09, Zn(II) = 0.88, Cu(II) = 0.87, and Ni = 0.83 Å) [36], the competitive adsorption capacity of the Cu(II)-IIP for Cu(II) ion is higher than the NIP (Table 4).

Multi-metal adsorption on the NIP and the Cu(II)-IIP was performed by SPE column technique with a flow rate around 0.32–0.35 mL/min (Fig. 9). The Cu(II)-IIP is more selective in separating Cu(II) from the multi-metal mixtures of Cu(II), Cd(II), Ni(II), Zn(II), Ag(I), and Ca(II) than the NIP (Fig. 8). On the Cu(II)-IIP, it can be observed that order of adsorbed metal ion tendency in the multi-metal solution follows these orders: Ca(II) < Cd(II) < Ni(II) < Zn(II) < Ag(I) < Cu(II).

Ag(I) is adsorbed relatively large but it is very hard to be released from the NIP and the Cu(II)-IIP (Fig. 9). Ag(I) ion is grouped as soft acid [36] and it has ionic size difference which is relatively larger from Cu(II) ion. In addition, it should not be adsorbed. However, in water, Ag(I) ion is very weak in a hydrate form and easy to interact with the active groups present on the Cu(II)-IIP. The Cu(II) ion has hydrate cation size of 1.96 Å. The existence of water molecules on $[Cu(H_2O)_6]^{2+}$ decreases the interaction of the Cu(II) ion with the active groups such as amine on the Cu(II)-IIP [37].

Table 3
Adsorption capacity of Cu(II) on several Cu(II) ionic imprinted polymer materials

Materials	Cu(II) adsorption capacity (mg/g)	Refs.
Ion-imprinted polymer based on salen-Cu complex	7.220	[11]
Double-imprinted polymer chitosan-Cu^{2+}	45.350	[12]
Cu(II)(poly(EGDMA-MAH/Cu(II))) microbead	48.000	[15]
Cu(II)-ion imprinted polymer from amino-silica	71.400	This work

Table 4
Adsorption competition of Cu(II), Cd(II), NI(II), Zn(II), and Ag(I) on NIP and Cu(II)-IIP (pH of 6.0; sample volume of 20 mL; temperature of 27°C)

	Adsorbents						
	Cu(II)-IIP			NIP			
	D (L/g)			*D* (L/g)			
Ion metal pairs	Cu(II)	M(II)	α	Cu(II)	M(II)	α	α_r
Cu(II)/Cd(II)	19.503	0.394	49.511	6.899	6.899	1.000	49.51
Cu(II)/Ni(II)	9.781	0.263	37.231	11.273	12.792	0.881	42.24
Cu(II)/Zn(II)	13.876	0.430	32.232	9.665	11.061	0.874	36.89
Cu(II)/Ag(I)	6.909	0.660	10.468	11.414	3.626	3.148	3.32

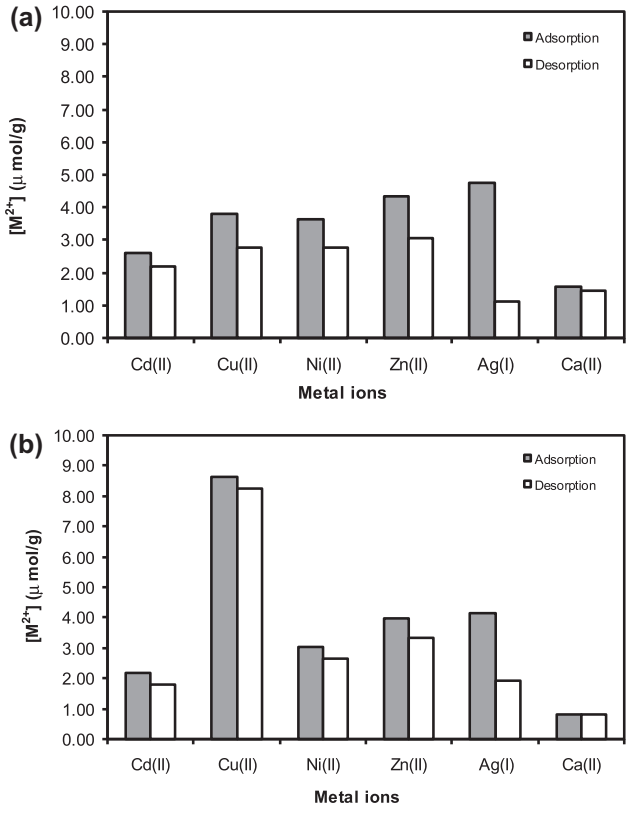

Fig. 9. Result of multi-metal adsorption–desorption in column system on (a) NIP and (b) Cu(II)-IIP.

3.7. Reusability

In order to study the reusing possibility, the material was used for several times to examine its ability in adsorbing experiment of Cu(II). The elution processes were carried out by shaking of the material in 40 mL of 0.1 M HCl and 0.1 M Na_2EDTA, for 30 min. The results show that adsorption ability of material decrease around 5% for five times toward first adsorption. Obviously, only very slight decrease of adsorption capacity occurred in recycling studies of the prepared Cu(II)-IIP material.

4. Conclusions

The Cu(II)-IIP from amino-silica hybrid obtained through simultaneous sol-gel process can be applied in Cu(II) separation from the matrix of other metal ions in solution, either as ionic pairs or multi-metal. The Cu-IIP material has the adsorption capacity and selectivity higher than the NIP material. The Cu-IIP material is very stable in acid condition and stable enough in neutral condition or rather base and it can be reused for five times with the reduction of adsorption ability around 5%.

Acknowledgments

The authors would like to thank to the Directorate of Research and Community Services, Directorate General of Higher Education (DIKTI), Ministry of National Education, Republic of Indonesia, for financial support of this research.

References

[1] R.J.E. Martins, R. Pardo, R.A.R. Boaventura, Cadmium (II) and zinc(II) adsorption by the aquatic moss *Fontinalis antipyretica*: Effect of temperature, pH and water hardness, Water Res. 38(3) (2004) 693–699.
[2] T.Y. Kim, S.Y. Cho, S.J. Kim, Adsorption equilibrium and kinetics of copper ions and phenol onto modified adsorbents, Adsorption 17 (2011) 135–143.
[3] J. Chung, J. Chun, J. Lee, S.H. Lee, Y.J. Lee, S.W. Hong, Sorption of Pb(II) and Cu(II) onto multi-amine grafted mesoporous silica embedded with nano-magnetite: Effects of steric factors, J. Hazard. Mater. 239–240 (2012) 183–191.
[4] A.Z.M. Badruddoza, A.S.H. Tay, P.Y. Tan, K. Hidajat, M.S. Uddin, Carboxymethyl-β-cyclodextrin conjugated magnetic nanoparticles as nano-adsorbents for removal of copper ions: Synthesis and adsorption studies, J. Hazard. Mater. 185 (2011) 1177–1186.
[5] Buhani, Suharso, Sumadi, Production of ionic imprinted polymer from *Nannochloropsis* sp biomass and its adsorption characteristics toward Cu(II) ion in solutions, Asian J. Chem. 24(01) (2012) 133–140.
[6] P.T. Rao, S. Daniel, J.M. Gladis, Tailored materials for preconcentration or separation of metals by ion-imprinted polymers for solid-phase extraction (IIP-SPE), Trends Anal. Chem. 23(1) (2004) 29–35.
[7] A. ErzÖz, R. Say, A. Denizli, Ni(II) ion-imprinted solid-phase extraction and preconcentration in aqueous solutions by packed-bed columns, Anal. Chim. Acta 502 (2004) 91–97.
[8] X. Chang, N. Jiang, H. Zheng, Q. He, Z. Hu, Y. Zhai, Y. Cui, Solid-phase extraction of iron(III) with an ion-imprinted functionalized silica gel sorbent prepared by a surface imprinting technique, Talanta 71 (2007) 38–43.
[9] Y. Zhai, Y. Liu, X. Chang, X. Ruan, J. Liu, Metal ion-small molecule complex imprinted polymer membranes: Preparation and separation characteristics, React. Funct. Polym. 68 (2008) 284–291.
[10] M.H. Arbab-Zavar, M. Chamsaz, G. Zohuri, A. Darroudi, Synthesis and characterization of nano-pore thallium (III) ion-imprinted polymer as a new sorbent for separation and preconcentration of thallium, J. Hazard. Mater. 185 (2011) 38–43.
[11] S. Walas, A. Tobiasz, M. Gawin, B. Trzewik, M. Strojny, H. Mrowiec, Application of a metal ion-imprinted polymer based on salen-Cu complex to flow injection preconcentration and FAAS determination of copper, Talanta 76 (2008) 96–101.
[12] E. Birlik, A. ErsÖz, A. Denizli, R. Say, Preconcentration of copper using double-imprinted polymer via solid phase extraction, Anal. Chim. Acta 565 (2006) 145–151.

[13] I. Dakova, I. Karadjova, I. Ivanov, V. Georgieva, B. Evtimova, G. Georgiev, Solid phase selective separation and preconcentration of Cu(II) by Cu (II)-imprinted polymethacrylic microbeads, Anal. Chim. Acta 584 (2007) 196–203.
[14] N.T. Hoai, D.K. Yoo, D. Kim, Batch and column separation characteristics of copper-imprinted porous polymer micro-beads synthesized by a direct imprinting method, J. Hazard. Mater. 173 (2010) 462–467.
[15] Y. Jiang, D. Kim, Effect of solvent/monomer feed ratio on the structure and adsorption properties of Cu^{2+}-imprinted microporous polymer particles, Chem. Eng. J. 166 (2011) 435–444.
[16] H. Liu, F. Yang, Y. Zheng, J. Kang, J. Qu, J.P. Chen, Improvement of metal adsorption onto *Chitosan/Sargassum* sp. composite sorbent by an innovative ion-imprint technology, Water Res. 45 (2011) 145–154.
[17] K. Wilson, A.F. Lee, D.J. Macquarrie, J.H. Clark, Structure and reactivity of sol-gel sulphonic acid silicas, Appl. Catal., A 228 (2002) 127–133.
[18] A. Kumar, Gaurav, A.K. Malik, D.K. Tewary, B. Singh, A review on development of solid phase microextraction fibers by sol-gel methods and their applications, Anal. Chim. Acta 610 (2008) 1–14.
[19] R.S.A. Machado, M.G. da Fonseca, L.N.H. Arakaki, J.G.P. Espinola, S.F. Oliveira, Silica gel containing sulfur, nitrogen and oxygen as adsorbent centers on surface for removing copper from aqueous/ethanolic solutions, Talanta 63 (2004) 317–322.
[20] N. Jiang, X. Chang, H. Zheng, Q. He, Z. Hu, Selective solid-phase extraction of nickel(II) using a surface-imprinted silica gel sorbent, Anal. Chim. Acta 577 (2006) 225–231.
[21] H. Yang, R. Xu, X. Xue, F. Li, G. Li, Hybrid surfactant-templated mesoporous silica formed in ethanol and its application for heavy metal removal, J. Hazard. Mater. 152 (2008) 690–698.
[22] M. Etienne, A. Walcarius, Analytical investigation of the chemical reactivity and stability of aminopropyl-grafted silica in aqueous medium, Talanta 59 (2003) 1173–1188.
[23] A.G.S. Prado, J.A.A. Sales, R.M. Carvalho, J.C. Rubim, C. Airoldi, Immobilization of 5-amino-1,3,4-thiadiazole-thiol onto silica gel surface by heterogeneous and homogeneous routes, J. Non-Cryst. Solids 333 (2004) 61–67.
[24] D. Pérez-Quintanilla, A. Sánchez, I. del Hierro, M. Fajardo, I. Sierra, Preparation, characterization, and Zn^{2+} adsorption behavior of chemically modified MCM-41 with 5-mercapto-1-methyltetrazole, J. Colloid Interface Sci. 313 (2007) 551–562.
[25] I. Zaręba-Grodź, W. Miśta, W. Stręk, E. Bukowska, K. Hermanowicz, K. Maruszewski, Synthesis and properties of an inorganic–organic hybrid prepared by the sol-gel method, Opt. Mater. 26 (2004) 207–211.
[26] Q. He, X. Chang, H. Zheng, N. Jiang, X. Wang, Determination of chromium(III) and total chromium in natural waters using a surface ion-imprinted silica gel as selective adsorbent, Int. J. Environ. Anal. Chem. 88(6) (2008) 373–384.
[27] N. Chiron, R. Guilet, E. Deydier, Adsorption of Cu(II) and Pb(II) onto a grafted silica: Isotherms and kinetic models, Water Res. 37 (2003) 3079–3086.
[28] R. Patel, S. Suresh, Kinetic and equilibrium studies on the biosorption of reactive black 5 dye by *Aspergillus foetidus*, Bioresour. Technol. 99 (2008) 51–58.
[29] N. Chen, Z. Zhang, C. Feng, M. Li, D. Zhu, N. Sugiura, Studies on fluoride adsorption of iron-impregnated granular ceramics from aqueous solution, Mater. Chem. Phys. 125 (2011) 293–298.
[30] M.M. Montazer-Rahmati, P. Rabbani, A. Abdolali, A.R. Keshtkar, Kinetics and equilibrium studies on biosorption of cadmium, lead, and nickel ions from aqueous solutions by intact and chemically modified brown algae, J. Hazard. Mater. 185 (2011) 401–407.
[31] Y.S. Ho, J.F. Porter, G. Mckay, Equilibrium isotherm studies for the sorption of divalent metal ions onto Peat: Copper, nickel, and lead single component system, Water Air Soil Poll. 141 (2001) 1–33.
[32] Buhani, Narsito, Nuryono, E.S. Kunarti, Production of metal ion imprinted polymer from mercapto-silica through sol-gel process as selective adsorbent of cadmium, Desalination 251 (2010) 83–89.
[33] W. Stumm, J.J. Morgan, Aquatic Chemistry, John Wiley and Sons, New York, NY, 1981.
[34] A.W. Adamson, Physical Chemistry of Surface, 5th ed., John Wiley and Sons, New York, NY, 1990.
[35] N. Atar, A. Olgun, S. Wang, Adsorption of cadmium (II) and zinc (II) on boron enrichment process waste in aqueous solutions: Batch and fixed-bed system studies, Chem. Eng. J. 192 (2012) 1–7.
[36] J.E. Huheey, E.A. Keiter, Inorganic Chemistry: Principles of Structure as and Reactivity, 4th ed., Harper, Collins Collage Publisher, New York, NY, 1993.
[37] A.E. Martell, R.D. Hancock, Metal Complexes in Aqueous Solutions, Plenum Press, New York, NY, 1996.